The Role of the Joint Panel Shear Deformation in Beam-to-Column Connections Part 2 : Numerical Analysis on Stress and Strain of Hot Spots

Rahiminia, Faramarz

Namba, Hisashi

Memoirs of the Graduate Schools of Engineering and System Informatics Kobe University
No. 5, pp. 1–6, 2013. doi:10.5047/gseku.e.2013.001

The Role of the Joint Panel Shear Deformation in Beam-to-Column Connections Part 2: Numerical Analysis on Stress and Strain of Hot Spots

Faramarz RAHIMINIA[1], Hisashi NAMBA[1]

[1]*Graduate School of Engineering, Department of Architecture*

(Received November 30, 2012; Accepted July 3, 2013; Online published July 10, 2013)

Keywords: *Joint Panel, Weld Access Hole, Crack Initiation, Stress Triaxiality, Equivalent Plastic Strain*

Following the observation of damages in experimental tests of fourteen full-scale beam-to-column sub-assemblies, this numerical investigation was conducted to understand the effect of joint panel strength ratio on crack initiation at hot spots. In order to study the stress and strain condition at hot spots, finite element analysis was performed using sub-modeling method. By comparison of crack indexes, it was evident that weak panel specimens are less critical for cracking compared to balanced and strong panel specimens. In balanced and strong panel specimens, the highest crack index was obtained for root of the weld access hole compared to other hot spots. In weak panel specimens, near same crack index was shown for all hot spots, however, experimental test observations revealed that root of the weld access hole is the most critical hot spot for cracking.

1. Introduction

Following the Northridge earthquake, based on observations and studies which had been undertaken within the SAC project, large joint panel shear deformation effect named "kinking" was recognized as one of the reasons for the brittle fractures in pre-Northridge moment resisting connections[1~4]; due to this approach in the US, the post-earthquake joint panel design provisions were modified to prevent excessive joint panel shear deformation[5]. Although this approach was supported by numerical and experimental investigations, reviewing the main related studies reveals that the role of the joint panel strength ratio had not been clearly addressed in those investigations. Within the SAC project, main numerical detail study was conducted by El-Tawil[3] which focused on cracking at root of the weld, while current experimental tests showed that root of the weld access hole is more critical hot spot for cracking. In the experimental and numerical analysis conducted by Ricles et al.[4], the range of joint panel strength ratios was limited to balanced and strong panel specimens in which the effect of joint panel strength ratio could not been well investigated.

In Japan, although in observations of damages of Kobe earthquake no premature brittle fracture due to the joint panel shear deformation was reported, the concerns about kinking effect were raised, as well. Kawashima et al.[6] could show the possibility of premature brittle fracture in weak panels just in specimens with very low toughness material properties. That investigation was conducted on specimens with shop welded joint detail and effect of joint panel strength ratio on field welded joint detail remained unknown.

This numerical analysis is a part of research program which was conducted aiming to improve the understanding of joint panel plastification behavior and its effects on elasto-plastic behavior of steel moment connections. This study focused on understanding the effects of joint panel strength ratio on crack initiation at hot spots which was done following the observation of damages in series of experimental tests which were reported in Part 1 of the paper[7]. For sake of simplicity in the modeling, the effect of HAZ on cracking was not considered in this study. Main parameters in this analytical study were the joint panel strength ratio and weld joint configuration of field welded and shop welded joint details.

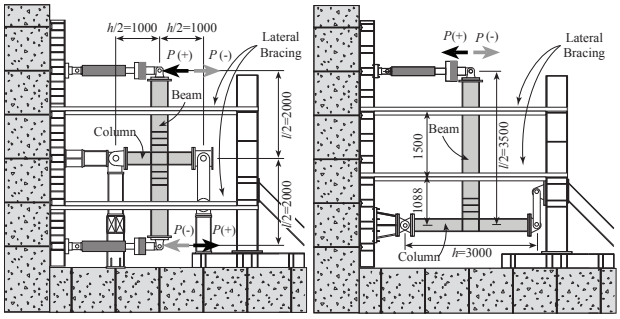

Fig. 1 Test setup

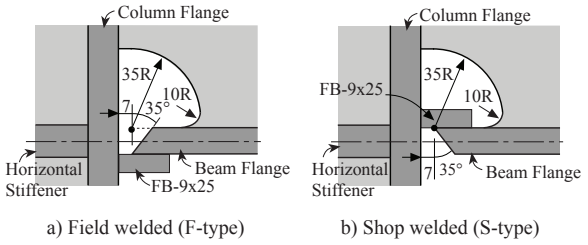

Fig. 2 Weld joint details

2. Detail Observation of Experimental Tests

In here, detail observations of failure of test specimens, reported in Part 1 of the paper[7] are newly discussed to show the detailed information of damages at hot spots. Table 1 presents the specification of specimens. and Figure 1 shows the test setup. The joint panel strength ratio ($_{pb}R_p$) of specimens changed from 0.47 to 1.42 with varying of doubler plate thickness. Sections of column and beam of specimens discussed here were H300x300x10x15 and H400x200x8x13 respectively for all specimens. $_{pb}R_p$ is given by ratio between the joint panel and beam full plastic strength.

Table 1 Experimental test specimen specification

Specimen ID	Members	Doubler plate	${}_{pb}R_p$	${}_{cb}R_p$	${}_c\kappa$	Weld joint
HE05S	Beam(SN490B): H-400×200×8×13 Column(SN490B): H-300×300×10×15	-	0.51	2.09	10	Shop S-type
HE08S		PL-6	0.81			
HE10S		PL-9	0.96			
HE11S		PL-12	1.09			
HE14S		2×PL-9	1.42			
HE06F	Beam(SM490A): H-400×200×8×13 Column(SM490A): H-300×300×10×15	-	0.59	2.52		Field F-type
HE10F		PL-6	0.96			
HE13F		PL-12	1.26			
HI06F		PL-9	0.60	1.32		
HI08F		PL-16	0.80			
HI10F		PL-9&12	0.97			
HI13F		2×PL-16	1.27			
HI05FW7	Beam(SM490A): H-400×200×12×19 Column(SM490B): H-300×300×16×22	PL-12	0.48	1.10	7	
HI05FW5	Beam(SM490A): H-400×200×12×19 Column(SM490B): H-300×300×16×28		0.47	1.41	5	

Specimens designed with two types of weld joint details of field (F-type) and shop (S-type) welded joint details as illustrated in Figure 2. More description regarding the specification of specimens can be found in 2.1 of Part 1 of the paper[7].

Based on pilot studies, three points were determined to be highly potential for cracking in field welded joint details (F-type) and shop welded joint details (S-type) as illustrated in Figure 3. For F-type specimens, observations on these hot spots were done using Macro-etch test from section of weld at center, after the loading tests. Careful observation by means of digital microscope was performed to find crack initiation and measuring the crack dimensions.

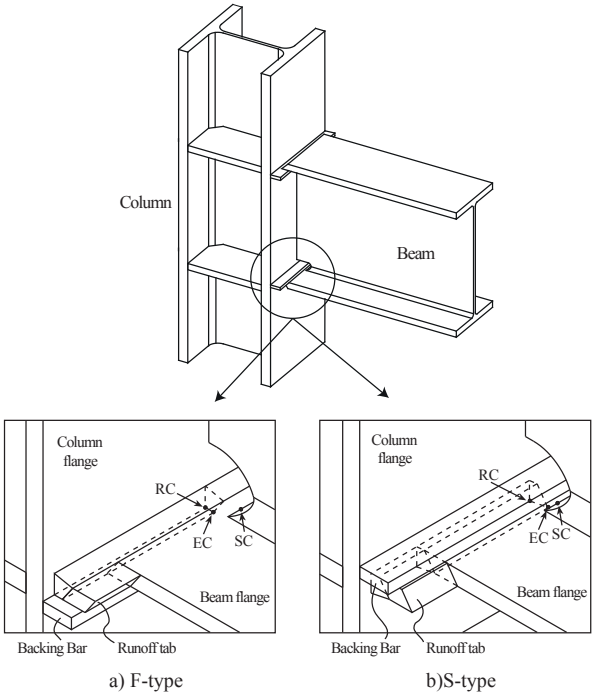

Fig. 3 Location of hot spots

2.1 Root of the weld access hole (SC)

2.1.1 First crack initiation

Figure 4 shows that for all specimens with different joint panel strength ratios (${}_{pb}R_p$) and weld joint details, in which loading cycle first crack initiation was observed. Crack initiation was defined when 0.2 mm crack opening was observed using a crack scale. As the chart shows, first crack initiation which happened at root of the weld access hole occurred at earlier stage of loading in strong and balanced panel specimens, shown with solid bars in the chart, compared to weak panel specimens shown by hollow bars.

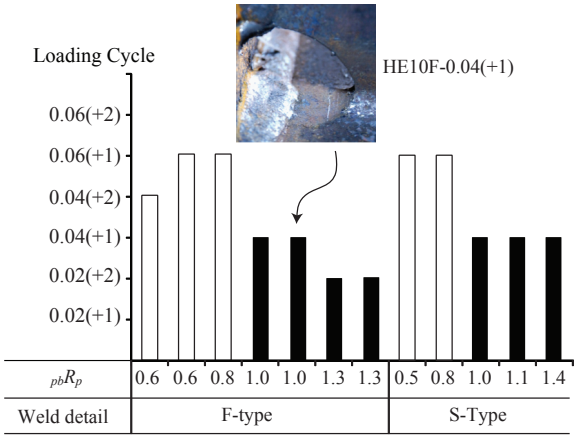

Fig. 4 First crack initiation during the loading test

2.1.2 Crack progress

Crack progress was investigated by plotting the measured crack opening (δ_{co}) verses total rotation as shown in Figure 5. In this Figure, (η_t) is the normalized total cumulative plastic rotation.

As can be seen in this graph, at same normalized total cumulative plastic deformation, the measured crack opening in weak panel specimens is less than balanced and strong panel specimens. A gradual increase of line slopes is shown by increase of joint panel strength ratio which indicates that in balanced and strong panel specimens crack growth has happened with higher speed compare to weak panel specimens.

2.2 Edge and root of the weld (EC and RC)

Observation of crack initiation at these two hot spots helped to find the effect of joint panel strength ratio on kinking of column and beam flanges.

In S-type specimens with shop welded joint detail, these hot spots were visible for observation during the loading test, which showed no detrimental crack initiation. Microscopic observations of Macro-etch tests conducted after the loading test from section of weld at center in F-type specimens, revealed a crack initiation from edge of the weld at center (EC) just in weak panel specimens as shown in Figure 6. This should be noted that this cracking in weak panel specimens was due to the very high amount of joint panel deformation. In these specimens, the normalized cumulative joint panel deformation (η_p) started from 294 for HI06F and reached to 878 for HE05S specimen. Considering the fact that for actual seismic application, these high amounts of joint panel deformations are not needed, this cracking is not so detrimental although it revealed the special care to avoid weld defects at root of the weld especially in weak panel specimens.

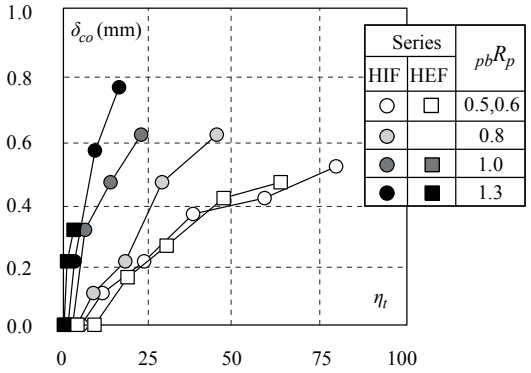

Fig. 5 Crack growth (δ_{co}- η_t)

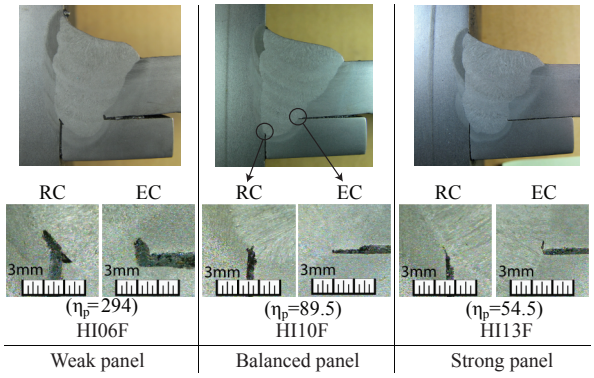

Fig. 6 Observation of section at center in HIF specimens

3. Numerical Analysis Specification

3.1 Outline of analysis

Among all the sub-assembling configurations in experimental test program, numerical analyses were conducted for a series of exterior column configuration with weak, balanced and strong joint panel design concepts aiming to investigate mechanical aspect of the effects of joint panel behavior on hot spots stress condition.

3.2 Modeling

In order to study the stress and strain condition at hot spots, sub-models for two types of shop (S-type) and field (F-type) welded joint details were developed using the results of global modeling. Finite element models were developed using the ABAQUS Ver.6.4.

3.3 Finite element global and sub-modeling

Figure 7 illustrates the configuration of finite element global and sub-models. The global model was composed of 4-noded thick shell elements and 2-noded beam elements and solid elements were employed in sub-models. Due to the symmetry half model was prepared. Considering that the backing bars had no set up welds in experimental tests, no contact action between backing bar and flanges was considered.

The monotonic loading applied upward and the sub-model placed in exact location of lower beam flange to column connection to implement the most critical condition. Results of global modeling were used in sub-modeling by defining the boundary condition of sub-model with equal displacement of corresponding global model.

Tensile test results on coupon tests for beam flange, column flange and weld metal are plotted in Figure 8(a) and the corresponding material models are shown in Figure 8(b).

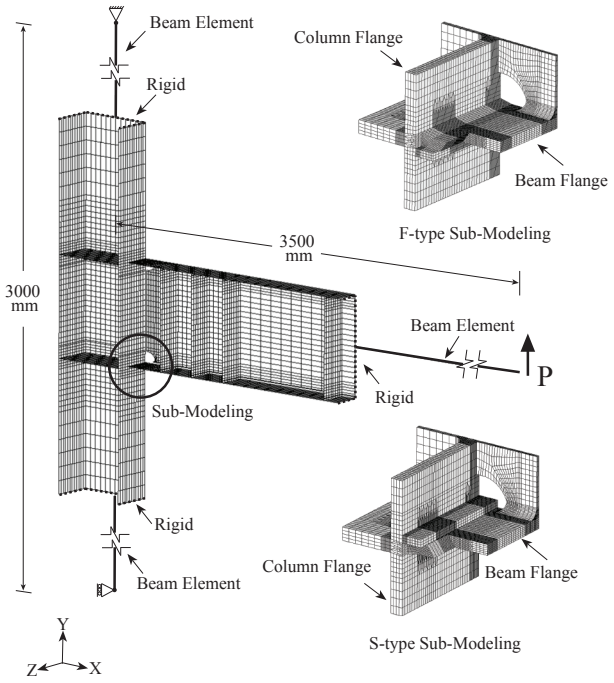

Fig. 7 Finite element global and sub-modeling

As it is shown in Table 2, four global models using the geometry and material properties of F-type experimental test specimens were provided. Therefore, detail study of S-type specimens performed on virtual specimens using HEF group material specification with shop welded joint detail as presented in Table 2.

Table 2 Global and sub-models specification

Global models	Sub-models	Members	Doubler plate	$_{pb}R_p$	$_{cb}R_p$
GHE06	SHE06F SHE06S	Beam(SM490A): H-400×200×8×13 Column(SM490A): H-300×300×10×15	-	0.59	2.52
GHE08	SHE08F SHE08S		PL-4	0.84	
GHE10	SHE10F SHE10S		PL-6	0.96	
GHE13	SHE13F SHE13S		PL-12	1.26	

3.4 Crack initiation criteria

Crack initiation criterion established by Kuwamura et al.[8] was used in this analysis. It is suggested that the initiation of the ductile crack is governed by three physical factors of strain, stress triaxiality and the uniform strain capacity of material. Based on this criterion, the strain level for crack initiation (e_c) is defined by Eq. (1), in which τ, and e_u are stress triaxiality and material uniform strain capacity, respectively.

$$e_c = e_u / \tau^2 \quad (1)$$

In this study a crack index defined by Eq. (2) were considered for comparison of crack potentiality at hot spots.

$$\text{Crack Index} = \text{PEEQ} / e_c \quad (2)$$

Where PEEQ is equivalent plastic strain.

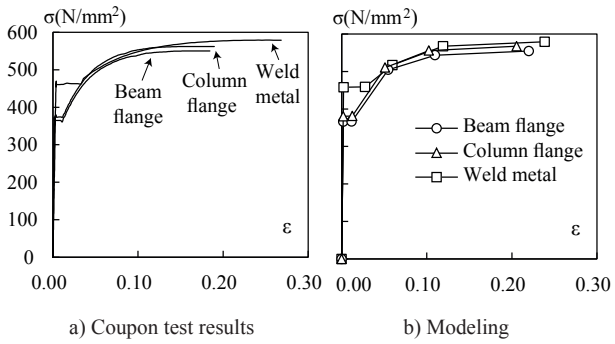

a) Coupon test results b) Modeling

Fig. 8 Material modeling

4. Numerical Analysis Results

4.1 Correspondence of modeling

Results of numerical monotonic loading are compared with skeleton curves obtained from experimental cyclic loading test for beam rotation in Figures 9(a) and (b) for weak (HE06), and strong (HE13) panel specimens, respectively. In these graphs the horizontal axis is beam component rotation (θ_b) normalized to beam plastic rotation capacity (θ_{bp}) and the vertical axis is beam moment at column face (M) normalized to beam full plastic capacity ($_bM_{bp}$). A graphical illustration for the beam component rotation is presented in Figure 4 of Part 1 of the paper[7]. For both specimens regardless of joint panel strength ratio, acceptable correspondence between numerical analyses and experimental test results can be observed.

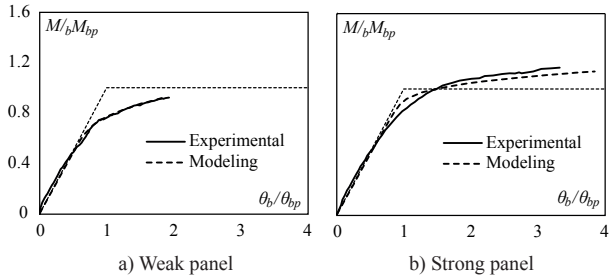

a) Weak panel b) Strong panel

Fig. 9 Correspondence of global model at total rotation

4.2 Plastic strain equivalent and beam rotation

Equivalent plastic strain (PEEQ) verses beam rotation is plotted in Figures 10(a), (c) and (d) for hot spots located at root of the weld access hole (SC), root of the weld at center (RC) and edge of the weld at center (EC), respectively. The locations of these three hot spots are shown in Figure 10(b) for different weld joint configurations of field welded (F -type) and shop welded (S-type) joint details.

The graphs show that generally at same beam deformation, higher strain demand is shown by reduction of joint panel strain ratio, especially at edge of the weld at center (EC) in Figure 10(d), greater effect of reduction of joint panel strength ratio can be observed. Strain level at root of the weld at center (RC) in Figure 10(c) is very small compared to other hot spots. No significant effect of weld joint detail can be observed for all hot spots.

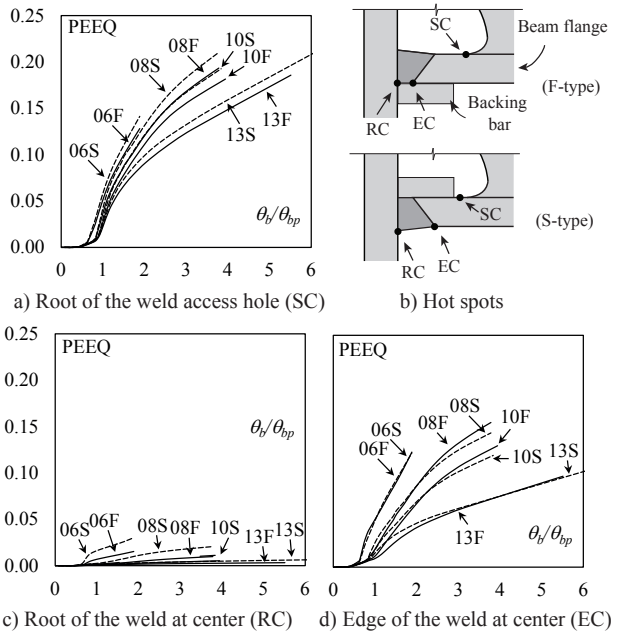

a) Root of the weld access hole (SC) b) Hot spots

c) Root of the weld at center (RC) d) Edge of the weld at center (EC)

Fig. 10 Strain demand at hot spots for beam rotation

4.3 Stress triaxiality and beam rotation

In Figures 11(a), (b) and (c) the level of stress triaxilaity is plotted for different beam rotations at three hot spots. Same amount of stress tiraxiality is shown in Figure 11(a) at root of the weld access hole (SC) for all specimens, regardless of joint panel strength ratio and weld joint details.

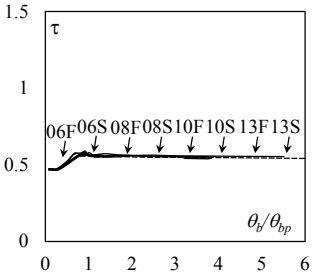

a) Root of the weld access hole (SC)

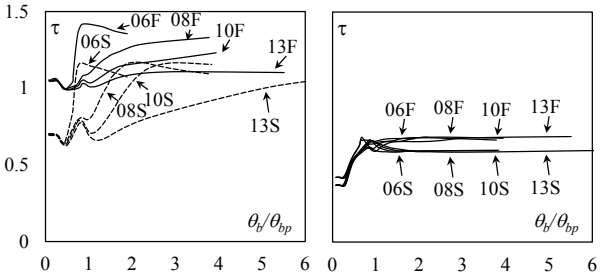

b) Root of the weld at center (RC) c) Edge of the weld at center (EC)

Fig. 11 Stress triaxiality condition of hot spots for beam rotation

At edge of the weld (EC) in Figure 11(c), same amount of stress triaxiality is obtained for different joint panel strength ratios. However, higher level of stress triaxiality is shown by field welded joint detail compared to S-type specimens which can be seen at root of the weld in Figure 11(b), as well. This might be related to higher constrain condition of this hot spot at F-type specimens because of the existence of backing bar as

can be seen in Figure 10(b). The level of stress triaxiality at root of the weld (RC) in Figure 11(b) is higher than other hot spots, especially in weak panel specimens with F-type weld joint detail, which is believed to be due to the kinking effect.

4.4 Crack index and beam rotation

Crack index values calculated based on Eq. (2), versus beam deformation are plotted in Figures 12(a), (b) and (c) for hot spots SC, EC and RC, respectively. Although the amount of crack index could not reach to one as the minimum value for crack initiation criteria, but the index could well compare the potentiality of cracking between hot spots. As it can be seen in all graphs, for same beam rotation, higher crack index is shown by reduction of joint panel strain ratio, especially at root (RC) and edge of the weld at center (EC) in Figures 12(b) and 12(c), greater effect of reduction of joint panel strength ratio can be observed. Figure 12(a) shows that weld joint detail has no effect on crack index at root of the weld access hole (SC), but in Figure 12(c), field welded joint detail specimens show higher crack index at edge of the weld at center (EC) because field welded joint detail specimens reached to higher level of stress triaxiality around 0.7 at this hot spot compared to shop welded joint detail specimens which showed lower stress triaxiality near 0.6 in Figure 11(c). In Figure 12(b), it can be seen that in weak panel specimens, crack index at root of the weld (RC) is marginally higher than other specimens regardless of small strain demand shown in Figure 10(c). This is because of high level of stress triaxiality at root of the weld (RC) in weak panel specimens shown in Figure 11(c), due to the kinking effect.

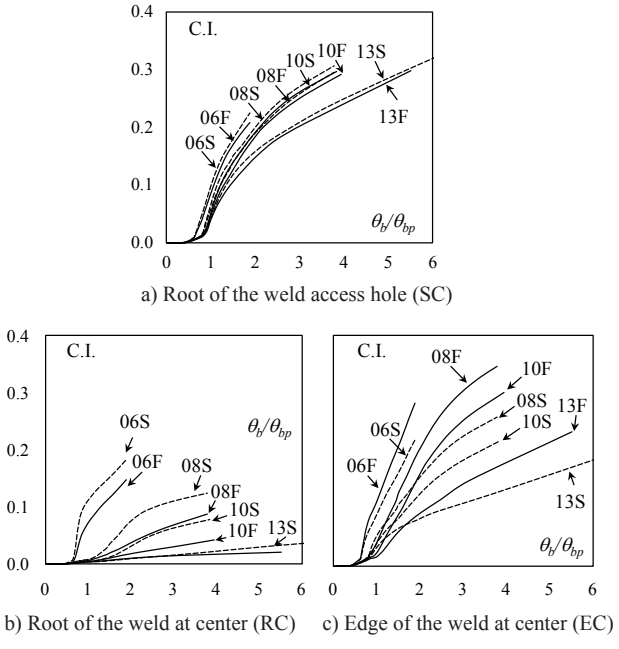

Fig. 12 Crack index at hot spots for beam rotation

5. Effect of Joint Panel on Hot Spots

In Figures 13, 14 and 15, equivalent plastic strain, stress triaxilality and crack index at hot spots for different joint panel strength ratios ($_{pb}R_P$) are plotted, respectively. These values are obtained at 0.06 rad total deformation angle.

5.1 Plastic equivalent strain

In total deformation, as the graph in Figure 13 shows, by reduction of joint panel strength ratio, the maximum strain demand which is at root of the weld access hole (SC), is reduced. This conditon at total rotation is opposite to what was shown for beam rotation in Figure 10(a), which reveals the role of contribution of joint panel deformation at weak panel specimens to the total deformation. This contribution could well decrase the strain demand at root of the weld access hole (SC) in weak panel specimens compared to balanced and strong panels.

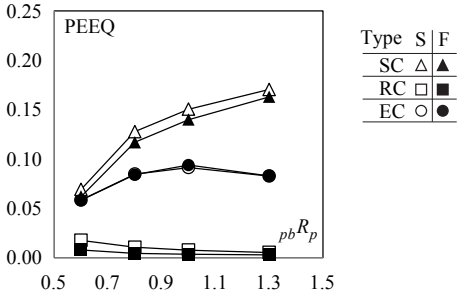

Fig. 13 Equivalent plastic strain at 0.06 rad total deformation

5.2 Stress triaxiality

Same stress triaxiality at root of the weld access hole (SC) is shown in Figure 14 for all specimens regardless of joint panel strength ratio and weld joint detail. Near same condition can be seen for edge of the weld (EC), however stress triaxiality at root of the weld (RC) is much higher than other hot spots especially for weak panel specimens with field welded joint detail.

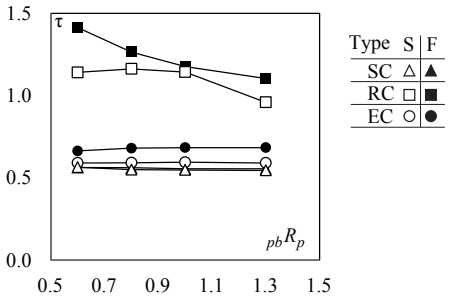

Fig. 14 Stress triaxiality at 0.06 rad total deformation

5.3 Crack index

Comparison of maximum crack index of specimens with different joint panel strength ratios in Figure 15 shows that by reduction of joint panel strength ratio, the maximum crack index of each specimen is reduced. This means that weak panels are less critical for cracking compared to balanced and strong panel specimens that is exactly in correspondence with what was found in experimental test detail observations reported in 2.1.

In weak panel specimens, near same value for crack index is obtained for all hot spots, however, detail observations of experimental tests described in 2.1 showed that root of the weld access hole (SC) is the most critical hot spot for cracking, even in weak panel specimens. As described in 2.2, in weak panel specimens due to very high amount of joint panel deformation, crack initiation was also observed from edge of the weld at center (EC). Here, (RC) has different condition compared to other hot spots. The high value of crack index for this hot spot is obtained by high level of stress triaxiality combined with very low level of strain demand

almost not in plastic region, which suggests the risk of brittle crack. This high level of stress triaxiality and crack index of this hot spot recommend the importance of soundness of weld metal at root layers of the weld, and also material toughness of column flange.

In balanced and strong panel specimens, root of the weld access hole (SC) gives higher crack index compared to other hot spots and different weld joint details of S-type and F-type had no effect on cracking from this critical hot spot. Experimental test observations reported in part 1 of the paper[7] also confirmed the high potentiality of cracking at root of the weld access hole (SC) with no effect of weld joint detail. It was observed that in all specimens regardless of weld joint detail first crack initiation was occurred at root of weld access hole (SC) and the basic failure mode in all specimens was crack propagation from this hot spot.

The effect of weld joint configuration can be clearly seen at edge of the weld at center (EC) for all specimens. At this hot spot F-type specimens show higher crack index which is due to the higher constraint condition because of the existence of backing bar.

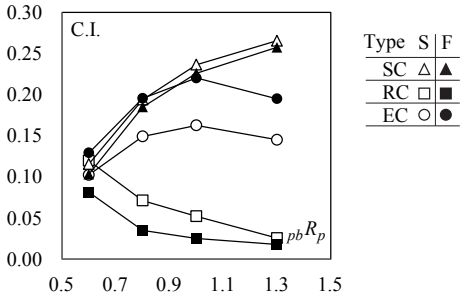

Fig. 15 Crack index at 0.06 rad total deformation

6. Conclusions

This numerical analysis was conducted to clarify the effect of joint panel strength ratio on cracking from potential hot spots at beam-to-column moment connections. The following conclusions are made:

- By comparison of crack indexes, it is evident that weak panel specimens are less critical for cracking compared to balanced and strong joint panel specimens.

-In balanced and strong joint panel specimens, the highest crack index was obtained for root of the weld access hole (SC) compared to other hot spots of root (RC) and edge (EC) of the weld at center. In weak panel specimens, near same crack index was shown for all hot spots.

- High stress triaxiality in root of the weld at center (RC) recommends the special note to the quality of weld at root layers and also material toughness properties of column flange especially in weak joint panel specimens.

- Different weld joint configurations of field welded (F-type) and shop welded (S-type) joint details, could affect the crack initiation form edge of the weld (EC), with higher crack index for F-type specimen.

Acknowledgement

The research described in this paper was supported by grants from Ministry of Education of Japan under the project No: 21560591, which is truly acknowledged.

Nomenclature

$_bM_{bp}$:	Theoretical beam plastic moment
$_bM_{pp}$:	Theoretical beam moment corresponding to joint panel yielding strength
$_{cb}R_p$:	Column to beam plastic strength ratio
e_c :	Crack initiation equivalent plastic strain
e_u :	Uniform strain of material
M:	Beam moment at column face
$_{pb}R_p$:	Joint panel to beam plastic strength ratio
δ_{co} :	Crack opening at tip of the weld access hole
η_b :	Normalized cumulative beam plastic rotation
η_p :	Normalized cumulative joint panel plastic rotation
η_t :	Normalized cumulative total plastic rotation
θ_b :	Beam contributed rotation angle
θ_{bp} :	Beam plastic rotation capacity
τ_{peak} :	Peak stress triaxiality

References

1) FEMA 350; “Recommended seismic design criteria for new steel moment-frame buildings, State of the art report on connection performance,” Federal Emergency Management Agency, Washington D.C. (2000)
2) FEMA 355D; “State of the art report on connection performance,” Federal Emergency Management Agency, Rep. FEMA 355D. Washington D.C. (2001)
3) El-Tawil, S.; “Panel zone yielding in steel moment connections,” *Eng. J. AISC*, 3qtr00,120-131 (2000)
4) Ricles J.M., J.W. Fisher, L.W. Lu and E.J. Kaufmann; “Development of improved welded moment connections for earthquake-resistant design,” *J. Const. Steel R.*, 58,565-604 (2002)
5) AISC Committee on Specifications; “Seismic provisions for Structural Steel Buildings,” ANSI/AISC 341-10. (2010)
6) Kawashima T., M. Tabuchi and T. Tanaka; “Effects of shear behaviour of column-to-beam joint panel on beam elastic-plastic behaviour,” AIJ Kinki Branch Annual Meeting:2050,213-216 (2000)
7) Rahiminia F. and H. Namba; “ The role of the joint panel shear deformation in beam-to-column connections Part 1: Results of the experimental test program,″ *Memories of the Graduate School of Engineering and System Informatics Kobe University*, No.4, 8-13 (2012)
8) Kuwamura H. and K. Yamamoto; “Ductile crack as trigger of brittle fracture in steel,″ *J. Struct. Eng. ASCE*, 123-6,729-735 (1997)